Supporting Information for

A Nano-Electro Mechanical Switch Based on a Physical Unclonable Function for Highly Robust and Stable Performance in Harsh Environments

Kyu-Man Hwang, [1,2] *Jun-Young Park,* [1] *Hagyoul Bae,* [1] *Seung-Wook Lee,* [1,3] *,Choong-Ki Kim,* [1] *Myungsoo Seo,* [1,3] *Hwon Im,* [1] *Do-Hyun Kim,* [1,4] *Seong-Yeon Kim,* [1,4] *Geon-Beom Lee,* [1] *and Yang-Kyu Choi* [1] *

[1] School of Electrical Engineering, 291 Daehak-ro, Korea Advanced Institute of Science and Technology (KAIST), Daejeon 34141, Korea.

[2] Semiconductor R&D Center, Samsung Electronics, Hwasung 18448, Republic of Korea

[3] System LSI Division, Samsung Electronics, Samsung-ro 1, Yongin-City, Gyeonggi-do, Korea

[4] SK hynix Inc. 2091 Gyeongchung-daero Bubal-eub Icheon-si, Gyeonggi-do, Korea

E-mail : ykchoi@ee.kaist.ac.kr

1. The differences in robustness between the previous silicon-based PUF and NEM-PUF

Unlike other silicon technology-based PUFs which rely on changes in electrical characteristics, NEM-PUF exploits the mechanical actuation of a SiNW and this intrinsic feature reinforce the robustness of the PUF to preserve data under various harsh environments. The differences in robustness between the previous silicon-based PUF and the proposed NEM-PUF are compared as follows :

[BER : Bit Error Rate]

	Si-based PUFs		**This work (NEM-PUF,** 288bits)	**Reference**
Condition	**Tested device**	**Device Failure after Stress**		
High Temperature	RRAM-PUF	BER 28% @400K, 24hr	BER 0% @423K, 24hr	[1]
	MRAM-PUF	BER 4~28% @300K		[2]
	SRAM-PUF	BER 14.06% @353K, 2hr		[3]
High Irradiation	Floating-gate flash	V_{th} shift 2.6V @550krad with *r*-ray	BER 0% @5Mrad with r-ray	[4]
	MOSFET (Silicon-on-insulator)	I_{off} increase by 6 orders @1Mrad with *r*-ray		[5]

Table S1. The differences in robustness between the previous silicon-based PUF and the proposed NEM-PUF.

2. Stiction Experiment of the NEM-PUF

A control experiment was designed to confirm the effect of liquid evaporation rate and drying direction on the randomness of the NEM-PUF, and it was experimentally proven that the symmetric stiction tendency is broken by asymmetric evaporation. When the sacrificial oxide (TEOS) was removed by a diluted HF solution and then dried, the drying speed on both sides of the SiNW became different by tilting the sample. In other words, the different amounts of the droplet along the tilted sample caused the direction of the SiNW stiction to be asymmetric. Because there was less liquid on the upper-side gate, it evaporated earlier, which also caused a smaller contact angle of the liquid on the solid surface. Consequently, stiction occurred more easily on the upper-side gate due to the stronger capillary force produced by the smaller contact angle. As a result, to implement randomness in the PUF, symmetric evaporation is preferred.

A comparison of the capillary forces caused by contact angle sizes is qualitatively predictable using the following equation[6,7] :

$$Capillary\ adhesion\ force = \pi R^2 \frac{2r\cos\theta_E}{H}$$

where R is the radius of the droplet forming the capillary force. H is the distance between the two plates, r is the surface tension, and θ_E is the contact angle, which is the angle measured between the solid surface and the liquid surface at the interface.

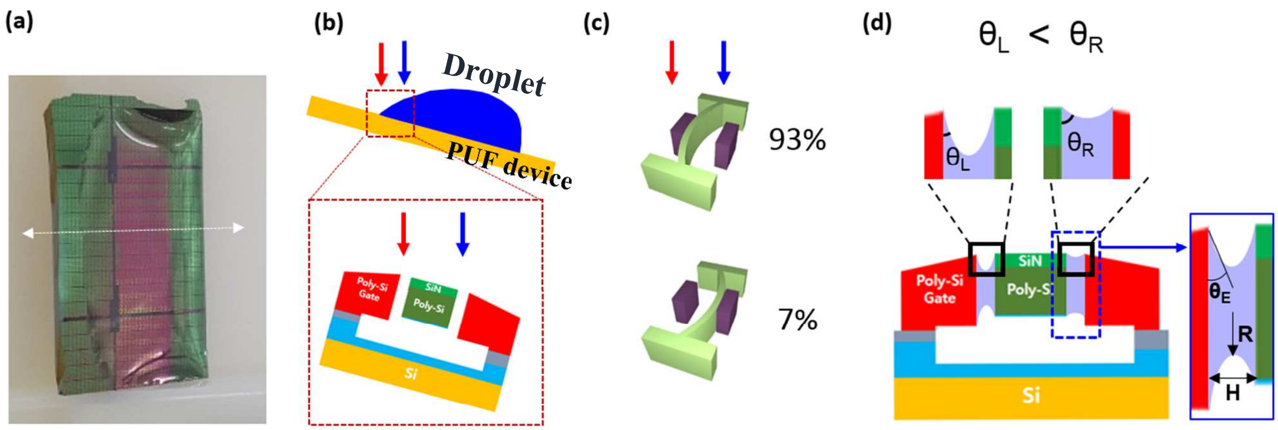

F (Adhesion force between two plates)

$$= \pi R^2 \frac{2r \cos \theta_E}{H}$$

(θ_E : contact angle
H : distance between two places
R : The radius of the droplet forming the capillary bridge
r : surface tension)

Figure S2. The asymmetric stiction induced by intentional oblique evaporation (a) optical photographic image (b) schematics (c) the asymmetric stiction ratio after natural drying (d) asymmetric capillary force depending on the difference in contact angle.

3. The implemented PUF array

The NEM switch PUF array is shown in Figure S1. Each cell of the device has a four terminal structure. A source or drain voltage can be applied to the SiNW, and a gate voltage is applied to each gate pad. A wider view of the PUF array was obtained by stitching together high magnification optical images.

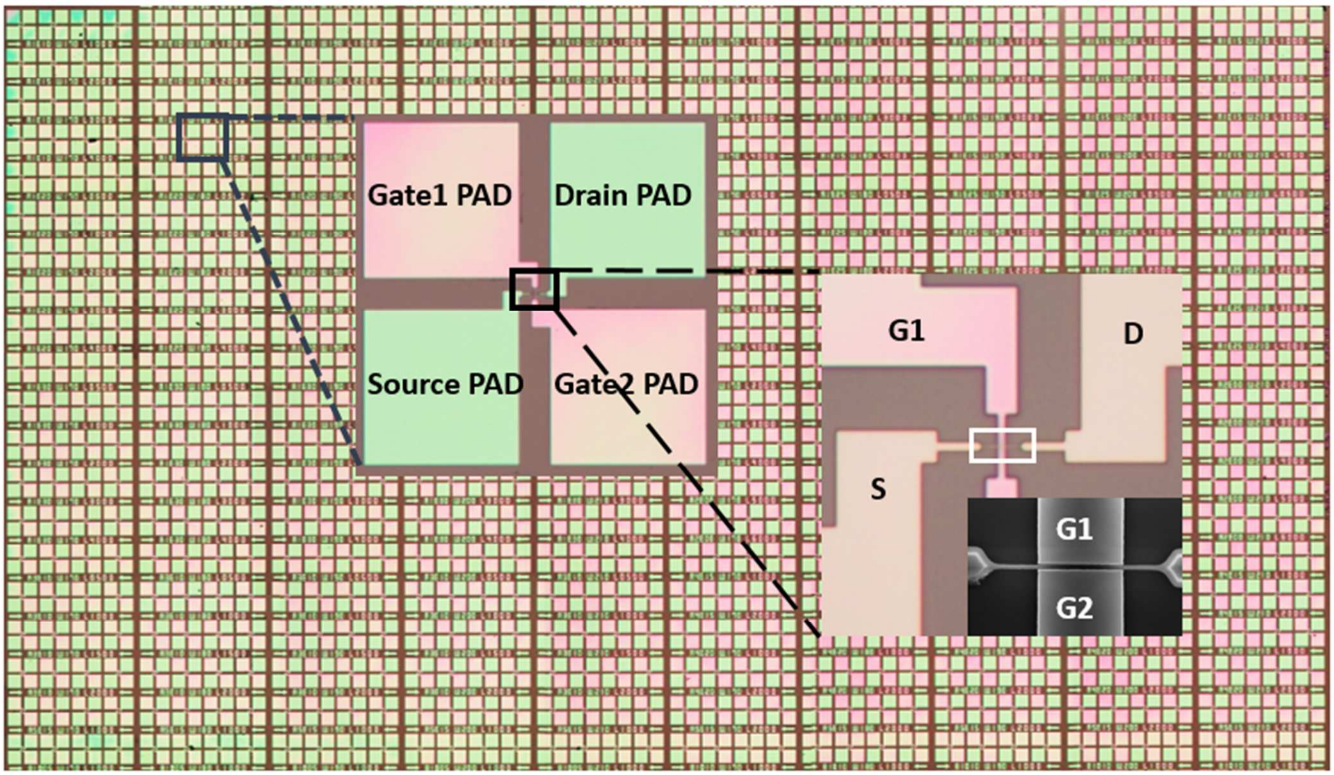

Figure S3. The implemented PUF array consisting of a SiNW and 4 pads. Each pad is connected to gate 1, gate 2, source, and drain.

4. Self-Destructible NEM-PUF for improved security against hacking

The NEM-PUF is robust and stable against harsh environments, meaning the stored data key cannot be easily changed. However, when the security chip is threatened by hacking or cloning, permanent device breakdown is required. To destroy the SiNW by mechanical static bending stress, a breakdown voltage was applied to the gate.[8] This self-destruction operation provides a useful option for the permanent destruction of the security device when it its faced with hacking and duplicating.

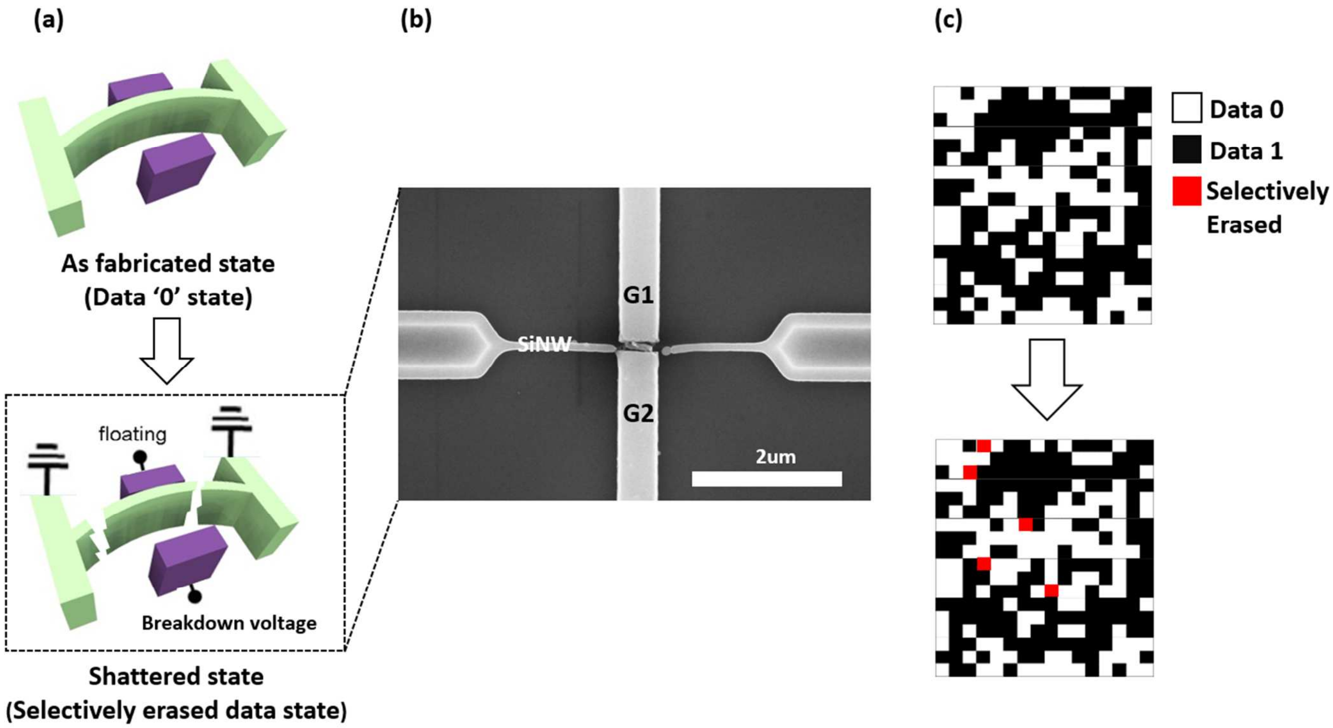

Figure S4. (a) Schematic illustration of an as-fabricated and self-destructed device (b) SEM image after the destruction action (c) Comparison of the data state before and after the destruction

5. Process flow of the Nano-Electro Mechanical Switch based PUF

A schematic of the fabricated NEM-PUF is presented in Figure S5. Ideally, if the thickness of the sacrificial oxide on both sides of the SiNW is equal, the probability of stiction occurring on either one is the same. The critical process to ensure random stiction is steps (f)~(g) of Figure S5, which are the etching of the sacrificial oxide and natural evaporation. First, the sacrificial oxide layer surrounding the SiNW (fin) and the BOX underneath the SiNW are removed with diluted HF solution (1 : 10 ratio of HF:DI water) during 5 minutes. Secondly, the sample is dipped in DI water for 10 min, and kept in a horizontal position when removed from the liquid. Lastly, the sample is placed on a flat floor and the liquid remaining in the sample is allowed to naturally evaporate in a windless environment. During this natural evaporation, stiction between the SiNW and gates occurs randomly.

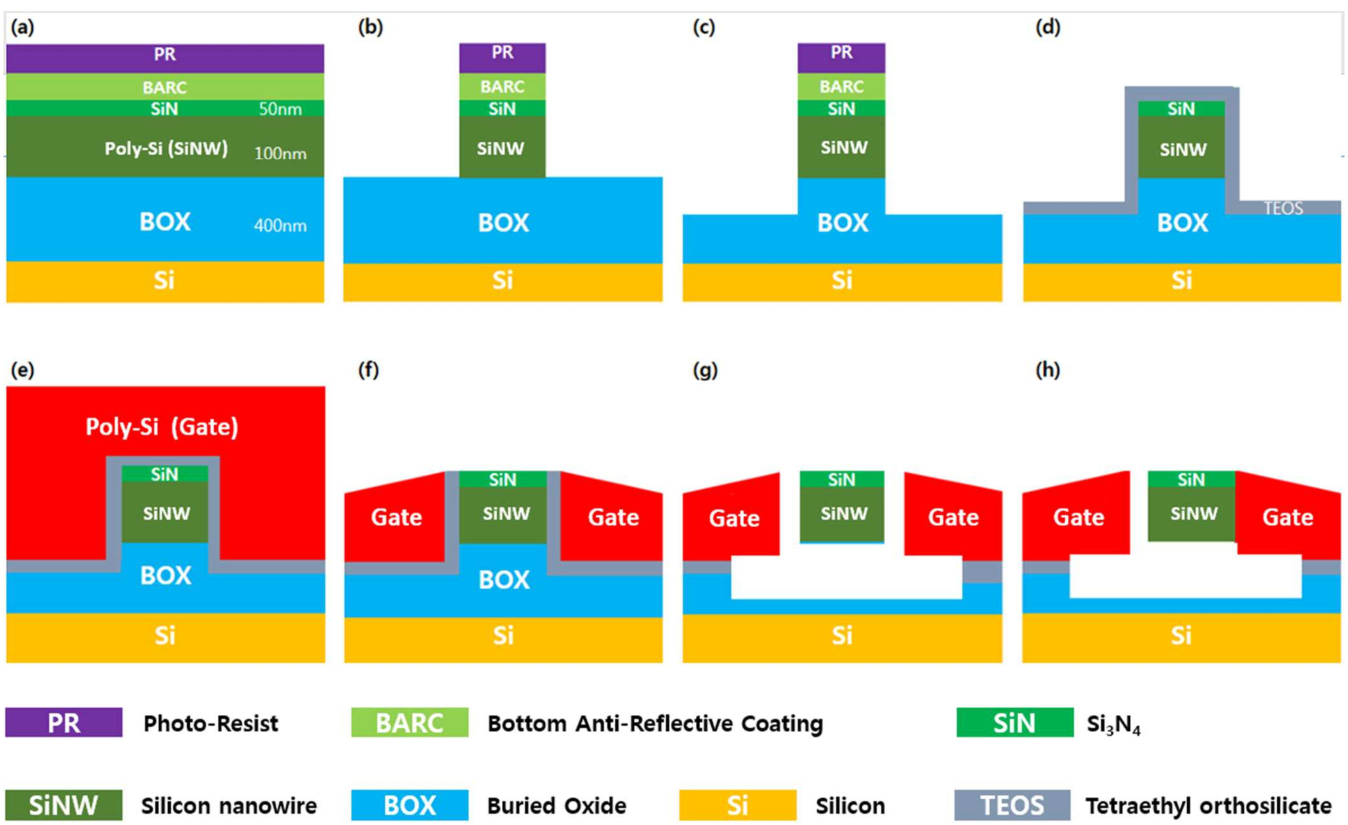

Figure S5. Fabrication process flow of the nano-electro mechanical switch based PUF device. (a) nitride deposition (50 nm) on silicon wafer (b) fin lithography, photoresist trimming and dry etching (c) dry etching for BOX (d) sacrificial TEOS oxide (15 nm) deposition (e) n^+ poly-Si (300 nm) deposition (f) chemical mechanical polishing with a stopping layer of nitride and gate poly-Si patterning (g) source/drain implantation and nanogap formation by TEOS oxide removal (i) inducing the stiction during a drying process

1. Chen, A. Utilizing the Variability of Resistive Random Access Memory to Implement Reconfigurable Physical Unclonable Functions. *IEEE Electron Device Lett.* **2015**, 36, 138-140.

2. Das, J., Scott, K., Rajaram, S., Burgett, D. and Bhanja, S. MRAM PUF: A Novel Geometry Based Magnetic PUF with Integrated CMOS. *IEEE Trans. Nanotechnol.* **2015**, 4, pp.436-443.

3. Xiao, K., Rahman, M.T., Forte, D., Huang, Y., Su, M. and Sehranipoor, M. Bit Selection Algorithm Suitable for High-Volume Production of SRAM-PUF. In *Hardware-Oriented Security and Trust (HOST), IEEE International Symposium on.* **2014**, (pp. 101-106). IEEE.

4. Cellere, G., Paccagnella, A., Visconti, A., Bonanomi, M., Candelori, A. and Lora, S. Effect of Different Total Ionizing Dose Sources on Charge Loss from Programmed Floating Gate Cells. *IEEE Trans. Nucl. Sci.,* **2005**, 52, pp.2372-2377.

5. Schwank, J.R., Shaneyfelt, M.R., Fleetwood, D.M., Felix, J.A., Dodd, P.E., Paillet, P. and Ferlet-Cavrois, V. Radiation Effects in MOS Oxides. *IEEE Trans. Nucl. Sci.,* **2008**, 55, pp.1833-1853.

6. Legtenberg, R.; Tilmans, H.A.; Elders, J. and Elwenspoek, M. Stiction of Surface Micromachined Structures after Rinsing and Drying: Model and Investigation of Adhesion Mechanisms. *Sens. Actuators, A*. **1994**, 43, pp.230-238.

7. De Gennes, P.G.; Brochard-Wyart, F. and Quéré, D. Capillarity and Wetting Phenomena: Drops, Bubbles, Pearls, Waves. *Springer Science & Business Media*. **2013**

8. Han, J.W.; Seol, M.L.; Choi, Y.K. and Meyyappan, M. Self-Destructible Fin Flip-Flop Actuated

Channel Transistor. *IEEE Electron Device Lett.* **2016**, 37, 130-133.